PHYSICAL REVIEW C VOLUME 23, NUMBER 6 JUNE 1981

Liquid drop model and heavy ion collisions

M. El-Nadi and A. Hashem
Faculty of Science, Cairo University, Giza, Cairo, Egypt
(Received 21 April 1980)

A macroscopic liquid drop model is considered in order to demonstrate the deep inelastic processes that take place in heavy ion collisions. The colliding nuclei, treated as two liquid drops, are assumed to form a single rotating and vibrating compound drop. This drop will either separate again into the parent nuclei, in addition to some smaller particles (satellites), or will form an equilibrium compound nucleus which decays either by particle evaporation or through fission. The maximum and minimum values of the critical angular momentum between which complete fusion occurs are calculated according to this model for several heavy ion reactions and good agreement with the experimental values is observed.

[NUCLEAR REACTIONS Heavy ion scattering; modified model for interaction of two liquid drops, its application to deep inelastic collisions between two heavy nuclei; calculations of critical angular momentum.]

I. INTRODUCTION

A new reaction mechanism was recently observed in heavy ion reactions in which the masses of the outgoing particles are in the vicinity of that of the target and projectile and where the bombarding energy is highly damped during collision.[1-8] This mechanism is called the "deep inelastic" or "quasifission" reaction. It was found that complete fusion of projectile and target nuclei takes place for a certain range of angular momenta, the two limits of which are called the critical angular momenta.[9-11] Several works were carried out to calculate the critical angular momentum. Wilczynski[12] and Bass[13] assumed that at the upper critical angular momentum the centrifugal and Coulomb repulsive forces are equal to the attractive nuclear force. For angular momenta less than the critical value the attractive nuclear force overcomes the repulsive forces and complete fusion occurs. The critical angular momentum calculated in this way is independent of the bombarding energy,[12] which contradicts the experimental observations.[14,15] Another classical approach to the determination of the upper critical angular momentum is to solve the equations of motion and find the maximum angular momentum corresponding to an orbit leading to complete fusion,[16,17] but the calculations are complicated. The nuclear potential used in all these methods is based on the liquid drop model. Recently, the proximity potential of Swiatecki[18] was considered to account for the nuclear interaction between heavy deformed nuclei.[18-22] The concepts of nuclear viscosity and friction losses were introduced to explain the energy dissipation.[2,7,23-27] Cohen *et al.*[28] studied the equilibrium configurations of a rotating charged liquid drop and calculated the critical angular momentum for complete fusion.

In the present work we shall assume a macroscopic liquid drop model for the nuclei and consider collision between two heavy nuclei as similar to the collision between two liquid drops and proceed to find the values of the two limiting angular momenta.

In Sec. II we shall give a short account of the collision between two liquid drops as developed by Brazier-Smith *et al.*[29] and Bradley and Stow[30] which will be followed in the present work. Some modifications of these methods are introduced so as to improve the agreement between the theoretical and experimental results for the collision between two liquid drops. In Sec. III the results derived in Sec. II are applied to the collision between two heavy nuclei. The existence of two critical angular momenta for complete fusion is clear in this model and good agreement is observed between the experimental and theoretical values of the critical angular momentum. In Secs. IV and V the results and conclusion are presented.

II. COLLISION BETWEEN TWO LIQUID DROPS

Experiments on collisions between water drops have shown a strong similarity to the collision between heavy nuclei. In particular it was found that there are upper and lower limits for the impact parameter between which permanent coalescence of the two colliding drops occurs.[30,31] For large impact parameters separation occurs due to high rotational energy and for small impact parameters separation occurs due to vibrational energy.[30,31] Methods were proposed to determine the stability criteria for the compound drop

formed after collision. Brazier-Smith *et al.*[29] calculated the upper critical value of the impact parameter of two colliding water drops. They assumed that the two charged drops form, after collision, an approximate spherically shaped rotating compound drop. At the same time complete mixing of the two drops does not occur.[29] Separation will occur, producing the parent drops, if the rotational energy plus the surface energy of the compound drop is equal to (or greater than) the surface energy of the outgoing drops. The results agreed with the experimental data,[29] although the vibrational energy of the compound drop and the rotational energy of the outgoing drops were neglected. Brazier-Smith *et al.*[29] found that—for the range of charges considered—the electrostatic energy effect was negligible. Moreover, it may be mentioned that the effects of the trapped air layer are negligible for high impact velocities.[31]

Bradley and Stow[30] adopted a graphical method for studying stability conditions of the compound drop. The expressions of energy of the colliding system are divided into two factors: one depends on the drop shape only while the other is shape independent. The relation between the shape dependent factors in the rotational and surface energies of the compound system defines a two dimensional curve which is called the parametric shape constraint (PSC) curve. Bradley and Stow[30] proposed that the colliding drops, during collision, form a rotating and vibrating compound system having the shape of an equipotential surface resulting from two equivalent point charges whose magnitudes are equal to the masses of the colliding drops and are located at their centers. The volume enclosed by this surface must be equal to the volume of the colliding drops if the liquid is incompressible. When the two centers coincide the equipotential surface becomes a sphere. It was then assumed that the compound system continues to vibrate, having an oblate configuration. Vibrations continue, following the assumed configurations, until complete mixing of the two drops occurs, unless disruption occurs during the first vibration. For this assumption the PSC curve will be in the form shown in Fig. 1, where—following same notation of Ref. 31—A_s and A_r are given by

$$A_s=\frac{E_s}{E_s^0}, \tag{1a}$$

$$A_r=\frac{E_r}{E_r^0}. \tag{1b}$$

E_s and E_r are the surface and the rotational energies of the composite system and E_s^0 and E_r^0 are

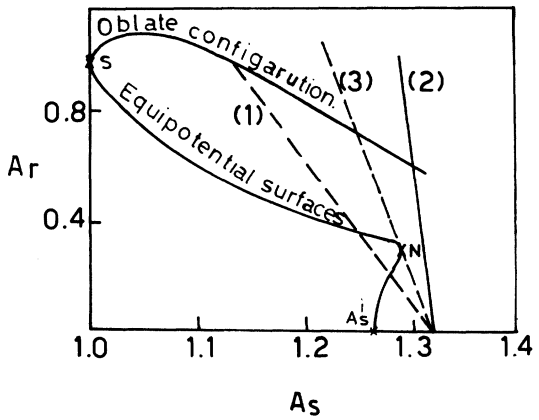

FIG. 1. Sketch of the parametric shape constraint curve for a composite system resulting from the collision of two equal drops (Ref. 30). The lower branch represents the configuration of equipotential surfaces. The upper branch represents the oblate configuration. The point S represents the spherical shape. The knee N represents the separation configuration. The lines 1, 2, 3 represent stable, unstable, and critically stable states of the composite drop, respectively.

the surface and the rotational energies of the corresponding spherical drop having the same angular momentum. The knee N of the PSC curve defines the separation configuration.

The total energy could be expressed in a dimensionless form by dividing all energies by the surface energy of an equivalent spherical drop. Neglecting Coulomb energy, the dimensionless total energy e_t is given by

$$e_t=A_s+e_rA_r+e_v, \tag{2a}$$

where e_r is the shape independent factor of the rotational energy, and is given by

$$e_r=\frac{E_r^0}{E_s^0}, \tag{2b}$$

and e_v is the dimensionless kinetic energy due to vibration; it will be referred to as the dimensionless vibrational energy.

At the extreme limits of oscillation the vibrational energy is zero.[30] Hence Eq. (2a) reduces to

$$e_t=A_s+e_rA_r. \tag{3}$$

The configurations at the limits of oscillation are determined by the points of intersection of the straight line in Eq. (3) (which is called the energy line) and the PSC curve. If there is one point of intersection only the compound drop is unstable because the configuration at the knee N would be reached during the oscillation. The lower critical impact parameter at certain energy e_t could be determined by drawing an energy line passing through the point $(e_t, 0)$ and tangent to the PSC

curve at the knee N, as shown in Fig. 1. In these calculations the angular momentum is assumed to be conserved. The experimental results for the lower critical impact parameter seem to disagree with the results calculated by this method even when energy loss due to viscosity is introduced.

To achieve agreement between the experimental and the theoretical results, we introduce the assumption that separation due to vibration will occur if the initial vibrational energy at collision (which arises from the radial velocity just at collision) is greater than or equal to a certain minimum value $e^i_{v\min}$. To determine this minimum value of energy, the case of head-on collision is considered. Applying conservation of energy at the instants of collision and separation one may have for the minimum initial vibrational energy

$$e^i_{v\min}=A^b_s-A^i_s, \tag{4}$$

where A^i_s and A^b_s are the dimensionless surface energies of the initial drops and those at breakup, respectively.

It is assumed that at this minimum value of energy the vibrational energy of the outgoing drops is zero. For noncentral collisions the minimum initial vibrational energy is given by

$$e^i_{v\min}=A^b_s-A^i_s-e_r(A^i_r-A^b_r), \tag{5}$$

where A^i_r and A^b_r are the shape dependent factors in the rotational energy at collision and breakup, respectively. e_r is given by Eq. (2b).

Taking the energy dissipated during collision into account and following the same method of Bradley and Stow,[30] Eqs. (4) and (5) reduce to

$$e^i_{v\min}=A^b_s-A^i_s+n(e_t-1), \quad \text{for central collision} \tag{6}$$

$$e^i_{v\min}=A^b_s-A^i_s-e_r(A^i_r-A^b_r)+n(e_t-1), \quad \text{for noncentral collisions} \tag{7}$$

where n accounts for energy losses due to viscosity and friction. $n(e_t-1)$ represents the energy losses during collision. It must be noticed that n here differs from the definition of n in Ref. 30, where the friction losses at collision and during neck formation were not considered.

The third term in the right-hand side of Eq. (7) represents the difference between the initial rotational energy of the system and the final rotational energy at the instant of separation when the dumbbell-shaped drop rotates as a rigid body. This term tends to reduce the minimum initial vibrational energy necessary to produce separation. At the same time it is expected that the centrifugal force causes the thickness of the neck of the compound drop to increase and hence the deformation at separation increases. Thus the knee of the PSC curve, which defines the shape at separation, is not fixed but its position changes according to the impact parameter and the bombarding energy. This differs from the previous work of Bradley and Stow,[30] where the knee was fixed. If the deformation increases, the energy loss during the neck formation increases also, i.e., A^b_s and n in Eq. (7) are larger than the same quantities in Eq. (6) at the same value of e_t. Hence, for small impact parameters (i.e., small e_r), the minimum vibrational energy may be approximated by Eq. (6), i.e., the difference between the rotational energy just at collision and the rotational energy at breakup balances the change occurring in the surface and dissipated energies.

To determine the lower critical impact parameter $X^{\text{low}}_{\text{crit}}$ at certain incident velocity u, conservation of energy is applied before and just at collision. Then one has

$$A^i_s+e_k=A^i_s+e^i_{v\min}+(e_r)^{\text{low}}_{\text{crit}}A^i_r, \tag{8a}$$

where e_k is the dimensionless bombarding energy in the center of mass system, $(e_r)^{\text{low}}_{\text{crit}}A^i_r$ is the dimensionless initial rotational energy corresponding to the lower critical impact parameter, and A^i_r is given by

$$A^i_r=\frac{\frac{2}{5}(m+M)(r^3+R^3)^{2/3}}{\frac{mM}{m+M}(r+R)^2}, \tag{8b}$$

where m, M and r, R are the masses and the radii of the colliding drops, respectively.

We define the Weber number N_{We} as[30]

$$N_{We}=\frac{\rho r}{\sigma}U^2, \tag{9}$$

where ρ is the density of the drop, σ is the surface tension, r is the radius of the incident drop, and U is the impact velocity.

Using Eqs. (6), (8a), (8b), and (9), and according to the definition of e_k, e_t, and e_r in Ref. 30, the lower critical impact parameter $X^{\text{low}}_{\text{crit}}$ for collision between two equal drops is given by

$$(X^{\text{low}}_{\text{crit}})^2=\frac{(1-n)e_t+n-A^b_s}{e_t-1.2599}, \tag{10}$$

where

$$e_t=\frac{N_{We}}{19.048}+1.2599 \tag{11}$$

and n in Eq. (10) is used as a fitting parameter whose value is determined from the experimental results of collision between water drops. To find an approximate value of n, the experimental results of Ref. 31 for collision between 300 μm drops are considered. It was found that the minimum velocity necessary to produce separation in central collision corresponds to $N_{We}^{1/2}\sim 7$.[30] The

outgoing drops are three drops [Fig. 7(a) of Ref. 31]. Assuming the three drops to be equal, then A_s^b is equal to 1.44; for unequal drops A_s^b will be smaller but the change is not large (e.g., for the case of two equal drops each of 80% of the mass of the original drop and a third drop whose mass is 40% of the original drop, A_s^b is 1.427). Hence, taking $A_s^b = 1.44$ and substituting in Eqs. (10) and (11) for $N_{We}^{1/2} = 7$ and $X_{crit}^{low} = 0$, we found that n equals 0.844. Substituting for $n = 0.84$ and $A_s^b = 1.29$ and 1.4 in Eqs. (10) and (11) the lower critical impact parameter could be determined as a function of $N_{We}^{1/2}$. The value of $A_s^b = 1.29$ corresponds to the knee of the PSC curve in Ref. 30. One may notice that A_s^b represents the dimensionless surface energy at separation in case of a head-on collision with minimum bombarding energy. The calculated values of X_{crit}^{low} are plotted versus $N_{We}^{1/2}$, and the results are shown in Fig. 2. The experimental data in this figure are taken from Ref. 30. In the same figure the calculated values of the lower critical impact parameter as calculated by Bradley and Stow[30] are presented. It is clear from Fig. 2 that the results obtained in the present work give better fitting to the experimental data. A refinement may be introduced by increasing n in Eq. (10) with bombarding energy. This is an acceptable assumption because the lower critical impact parameter increases with the bombarding energy, so the deformation and hence the friction loss both increase. The increase in energy dissipation may be so large that the initial rotational energy is insufficient to balance it.

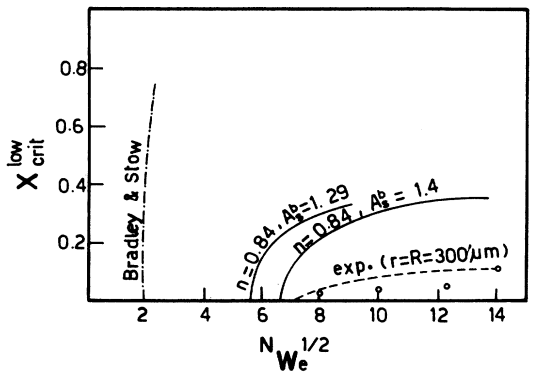

FIG. 2. The relation between the lower critical impact parameter X_{crit}^{low} and $N_{We}^{1/2}$. The dashed-dotted curve represents the results of Bradley and Stow (Ref. 30). The solid curves represent the results obtained according to the new method taking $n = 0.84$ and $A_s^b = 1.4$, 1.29. The dashed curve represents the experimental data as obtained from Ref. 30.

III. DEEP INELASTIC COLLISION

Applying the model used for the collision of two liquid drops to the case of the collision of two nuclei, we shall assume that after collision a rotating and vibrating complex system is formed in which each nucleus preserves its identity for a small number of oscillations. Separation will occur during the first cycle, either due to vibration for low partial waves or due to rotation for high partial waves. To determine the upper and lower critical angular momenta between which complete fusion occurs, the same precedure adopted in Sec. II will be applied but the Coulomb energies are introduced. Thus, similar to Eqs. (6) and (8a) the minimum initial vibrational energy and the lower critical angular momentum will be given by

$$E_{v_{min}}^i = E_D + X_{CB}^b - X_{CB}^i + \Delta E \tag{12}$$

and

$$\hbar^2 (X_{crit}^{low})^2 = (\eta E - E_D - X_{CB}^b)[2\mu(r+R)^2], \tag{13}$$

where E_D is the deformation energy, given by

$$E_D = E_s^b + E_c^b - E_s^i - E_C^i, \tag{14}$$

ΔE is the energy dissipated in one cycle after collision, given by

$$\Delta E = (1-\eta)E, \tag{15}$$

μ is the reduced mass, r, R are the radii of the interacting nuclei, E_s, E_C, and X_{CB} are the surface and Coulomb energies and the Coulomb barrier, respectively, i and b refer to the state just at collision and at separation, respectively, E is the bombarding energy in the center of mass system, and η is a fractional fitting parameter to account for the energy remaining after dissipation.

The upper critical angular momentum is calculated according to the method of Brazier-Smith *et al.*[29] applied to the case of a collision between water drops, but the outgoing nuclei are assumed to be deformed. In this case the vibrational energy of the compound nucleus at the instant it takes the spherical shape is assumed to be equal to the rotational energy of the outgoing nuclei plus the energy dissipated during collision. This assump tion is supported by the good results obtained in the case of collision between water drops.[29,30] Thus, the rotational energy $(E_r)_{crit}$ of the spherical composite system corresponding to the upper critical angular momentum l_{crit}^{up} will be given by

$$(E_r)_{crit} = E_s^b + E_C^b + X_{CB}^b - E_s^0 - E_C^0, \tag{16}$$

where E_s^0 and E_C^0 are the surface and Coulomb energies of the spherical system.

The upper critical angular momentum will be given by

$$\hbar^2(l_{\rm crit}^{\rm up})^2=\tfrac{4}{5}(E_r)_{\rm crit}\ (M+m)(r^3+R^3)^{2/3}, \tag{17}$$

where M, m are the masses of the two colliding nuclei and r, R are their radii.

To find the values of E_s^b and E_C^b in Eqs. (14) and (17) a specific configuration for the compound system at breakup must be assumed. The dumbbell-shaped nucleus which exists just before separation may be approximated by two prolates of the same ratio of axes.

The minimum bombarding energy $E_{\rm min}$, below which separation due to rotation does not occur, is the energy at which the upper critical angular momentum equals the grazing angular momentum, assuming the outgoing nuclei to be undeformed. Hence $E_{\rm min}$ will be given by

$$E_{\rm min}=X_{\rm CB}^i+\hbar^2(l^2)_{\rm crit}^{\rm up}/[2\mu(r+R)^2]. \tag{18}$$

IV. CALCULATIONS AND DISCUSSION

Equations (13) and (17) are used to calculate the upper and lower critical angular momenta. The surface energy, the Coulomb energy, and the rotational energy of a spherical nucleus with atomic number Z, mass number A, and angular momentum $\hbar l$ are given by[28]

$$E_s=17.9439\left[1-1.7826\left(\frac{A-2Z}{A}\right)^2\right]A^{2/3}\ \text{MeV}, \tag{19}$$

$$E_C=0.7053\frac{Z^2}{A^{1/3}}\ \text{MeV}, \tag{20}$$

$$E_r=34.54\frac{l^2}{A^{5/3}}\ \text{MeV}. \tag{21}$$

The radius parameter r_0 in these equations is taken as 1.2249 fm.

For the prolate configuration of ratio of axes γ ($\gamma>1$), the surface and Coulomb energies are given by[30]

$$E_s'=\tfrac{1}{2}E_s\gamma^{-2/3}\left[1+\frac{\gamma}{(1-1/\gamma^2)^{1/2}}\arcsin(1-1/\gamma^2)^{1/2}\right], \tag{22}$$

$$E_C'=E_C\frac{\gamma^2}{3\left\{\dfrac{1}{2(1-1/\gamma^2)^{3/2}}\ln\left[\dfrac{1+(1-1/\gamma^2)^{1/2}}{1-(1-1/\gamma^2)^{1/2}}\right]-\dfrac{1}{1-1/\gamma^2}\right\}}, \tag{23}$$

where E_s and E_C are given by Eqs. (19) and (20). The Coulomb barrier at separation is given by

$$X_{\rm CB}^b=\frac{X_{\rm CB}^i}{\gamma^{2/3}}, \tag{24}$$

where

$$X_{\rm CB}^i=\frac{1.44Zz}{r+R}. \tag{25}$$

Z and z are the atomic number of the colliding nuclei.

The critical angular momentum for complete fusion, at certain energy, is given by

$$l_{\rm crit}^2=(l_{\rm crit}^{\rm up})^2-(l_{\rm crit}^{\rm low})^2. \tag{26}$$

If $l_{\rm crit}^{\rm up}$ is greater than the grazing angular momentum $l_{\rm gr}$, then Eq. (26) reduces to

$$l_{\rm crit}^2=l_{\rm gr}^2-(l_{\rm crit}^{\rm low})^2. \tag{27}$$

The experimental values of the critical angular momentum for different nuclear reactions are taken from Table I in Ref. 10.

It was found that when $r_0=1.2249$ fm the experimental values of the critical angular momentum, for many reactions near the Coulomb barrier, exceeds the grazing angular momentum. This may be attributed to deformation in the nuclei before collision due to strong Coulomb interaction. This suggests taking r_0 as 1.44 fm. When the calculations of the critical angular momentum were repeated using $r_0=1.3$ fm, the results slightly changed but the main features of the model were unchanged. It may be more convenient to assume that the two interacting nuclei are deformed before collision and have the oblate configuration instead of the spherical shape which implies the use of a large radius parameter.

The ratio of axes γ, which is used to determine E_s^b and E_C^b in Eq. (16)—i.e., corresponding to the upper critical angular momentum—is denoted by $\gamma_{\rm up}$. Similarly, the ratio of axes γ, which is used to determine E_s^b and E_C^b in Eq. (14)—i.e., corresponding to the lower critical angular momentum—is denoted by $\gamma_{\rm low}$. Taking η in Eq. (13) as 0.9, one may proceed to obtain an empirical formula for the ratio of axes $\gamma_{\rm low}$, corresponding to the lower critical angular momentum by considering all the reactions where the ratio of masses (mass numbers) of the interacting nuclei are approximately the same. For each reaction the critical angular momentum is calculated by changing $\gamma_{\rm up}$ and $\gamma_{\rm low}$ in steps of 0.01. For each value of $\gamma_{\rm up}$, $\gamma_{\rm low}$ is changed until good fitting to the experimental values of the critical angular momentum is obtained. The critical angular momentum is calculated using Eqs. (13)–(17) and (19)–(26). In the reactions where $E<E_{\rm min}$, where $E_{\rm min}$ is given by Eq. (18), there is no separation due to rotation and $l_{\rm crit}^{\rm up}$ has no meaning. In this case Eq. (27) is used to determine the critical angular momentum instead of Eq. (26) and there is only one value of $\gamma_{\rm low}$ at which the calculated critical angular momentum and the experimental one agree. Plotting

the values of γ_{low} which give good fitting to the experimental data versus $(E - X^i_{CB})/X^i_{CB}$ for the reactions of nearly the same ratio of mass numbers of the colliding nuclei, A_1/A_2, the relation could be approximated by a straight line as shown in Fig. 3. Hence γ_{low} may be given by

$$\gamma_{low} = a \frac{E - X^i_{CB}}{X^i_{CB}} + b , \tag{28}$$

where a and b are functions of A_1/A_2 (>1). For each value of A_1/A_2 the parameters a and b in Eq. (28) are determined from Fig. 3. It is clear, from this figure, that γ_{low} decreases as A_1/A_2 increases for the same value of $(E - X^i_{CB})/X^i_{CB}$.

The relations between a and b and A_1/A_2 are approximated by straight lines [Fig. (4)]. By using the least square fitting method a and b were found to be given by

$$a = -0.011\,82(A_1/A_2) + 0.166\,46 , \tag{29}$$

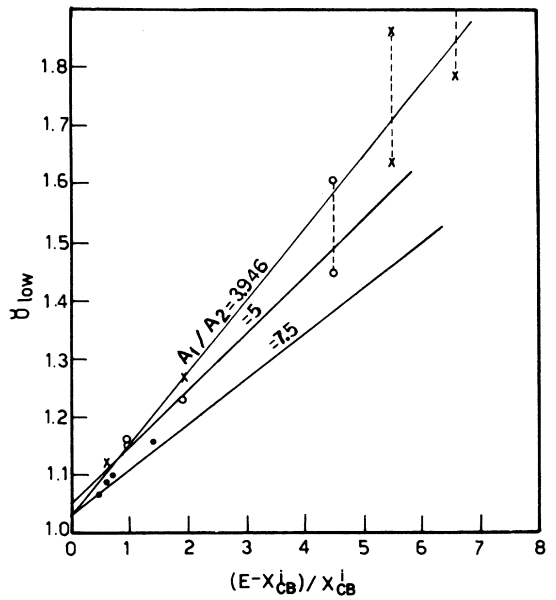

FIG. 3. The relation between γ_{low} and $(E-X^i_{CB})/X^i_{CB}$. The solid circles represent the reactions N+Rh (72 and 106 MeV), N+Ag (69 MeV), and Ne+Nd (127 MeV) where the ratio of mass numbers, A_1/A_2, is about 7.5. The hollow circles represent the reactions C+Ni (53 and 149 MeV) and C+Cu (54 and 81 MeV) where $A_1/A_2 \simeq 5$. The crossed points represent the reactions C+Ti (65 and 144 MeV), Ar+Ho (241 MeV), and N+Cr (206 MeV) where $A_1/A_2 \simeq 3.946$. For the reactions where $E > E_{min}$, the range of values of γ_{low}—each corresponding to a certain γ_{up}—which gives good fitting to the experimental data, is indicated by dotted lines. The straight lines represent the approximated relation between γ_{low} and $(E-X^i_{CB})/X^i_{CB}$ for the reactions having the same value of A_1/A_2. The experimental data are taken from Ref. 10.

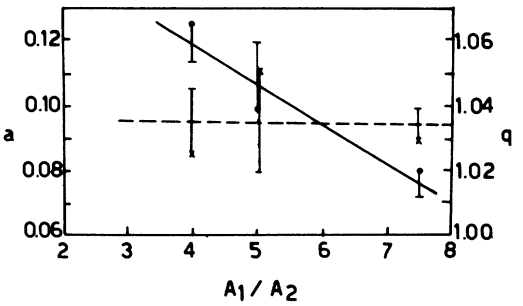

FIG. 4. The values of a (●) and b (×) in Eq. (28)—as determined from Fig. 3—are plotted versus the corresponding value of A_1/A_2. The solid line represents the approximated relation between a and A_1/A_2 which is given by Eq. (29). The dashed line represents the approximated relation between b and A_1/A_2 which is given by Eq. (30). The vertical lines represent the errors in determining the values of a and b from Fig. 3.

$$b = -0.000\,294(A_1/A_2) + 1.0366 . \tag{30}$$

Then for all nuclear reactions given in Table I in Ref. 10—except Kr induced reactions—where $E < E_{min}$, i.e., where separation occurs due to vibration only, the critical angular momentum is determined by using Eqs. (13)–(15), (19)–(25), and (27), where γ_{low} is determined from the empirical equations (28), (29), and (30). The calculated values of the critical angular momentum are plotted versus the experimental values; the results are represented by the solid circles in Fig. 5. An agreement between them is observed.

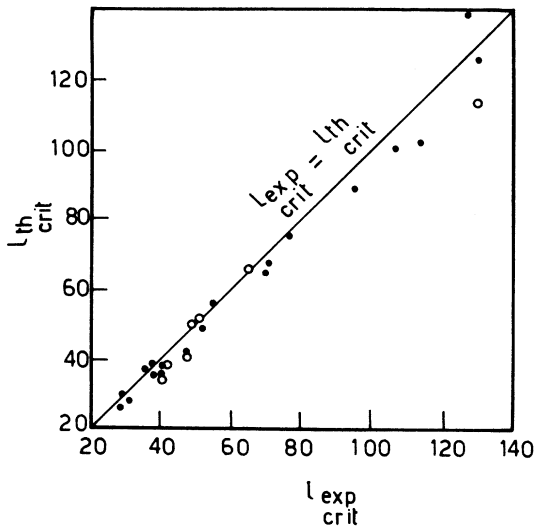

FIG. 5. The relation between $l_{th,crit}$ and $l_{exp,crit}$ for the reactions in Table I of Ref. 10 (except the Kr induced reactions). The solid circles represent the reactions where $E < E_{min}$. The hollow circles represent the reactions where $E > E_{min}$. The straight line represents the case when $l_{th,crit} = l_{exp,crit}$.

The calculations of γ_{low} are repeated, taking η in Eq. (13) as 0.6, 0.7, and 0.8. The results for the reactions where A_1/A_2 equal 5 and 7.5 are shown in Figs. 6 and 7. Comparing these figures to Fig. 3, it is clear that the only change due to changing η is that γ_{low} decreases with η, i.e., according to Eq. (15), when the energy losses increase. Relations similar to Eq. (28) may be obtained for each value of η.

The increase of γ_{low} with incident energy means, according to Eqs. (12), (22), and (23), that the minimum initial vibrational energy is not fixed but increases with energy. It may be more convenient to assume that this increase in the energy necessary to produce separation due to vibration is also due to the large increase in the energy dissipated during collision. Assuming η decreases with increasing energy [i.e., according to Eq. (15) the energy loss increases], the change in γ_{low} with energy will be smaller than the case where η is kept constant. This is clear in Figs. 6 and 7 where η is taken as 0.9 for the smallest energy and decreases to 0.6 (or 0.7) for the largest energy. This is more acceptable because E_D in Eq. (13) represents the minimum deformation corresponding to central collision which must be fixed. The increase in the minimum initial vibrational energy may be mainly due to the large increase in energy losses which cannot be balanced by the rotational energy as discussed before in Sec. II.

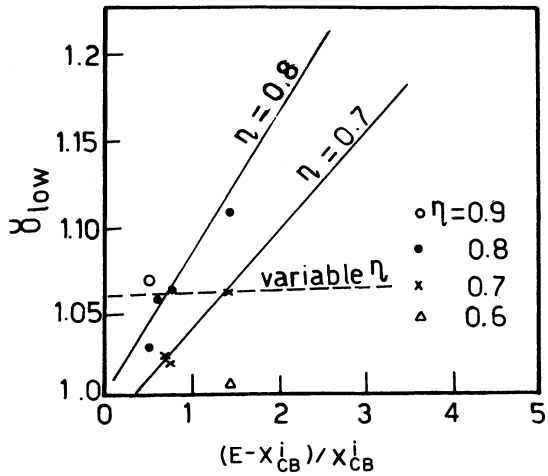

FIG. 6. The same as Fig. 3 for reactions where $A_1/A_2 = 7.5$ but for different values of η in Eq. (13). When η is taken as 0.6 no fitting was obtained except for N+Rh at 106 MeV. The dashed line represents the relation between γ_{low} and $(E-X^i_{CB})/X^i_{CB}$ when η is assumed to be decreased as the incident energy increases; i.e., for the smallest $(E-X^i_{CB})/X^i_{CB}$, η is taken to be 0.9, for the largest $(E-X^i_{CB})/X^i_{CB}$, η is taken to be 0.7. The point (○) represents the case where $\eta = 0.9$ at the smallest energy only.

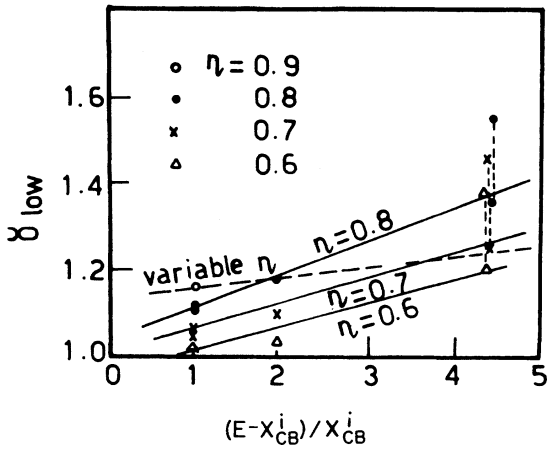

FIG. 7. The same as Fig. 6 but for $A_1/A_2 = 5$.

The values of γ_{low} when η is variable may give a better idea about the deformation in the outgoing nuclei than in the case when η is kept constant.

The minimum incident energy E_{min} necessary to produce separation due to rotation is determined for most of the reactions in Ref. 10 by using Eq. (18). The calculated values are plotted versus the ratio of mass numbers of the colliding nuclei; the results are presented in Fig. 8.

To determine l_{crit} in the case of reactions—in

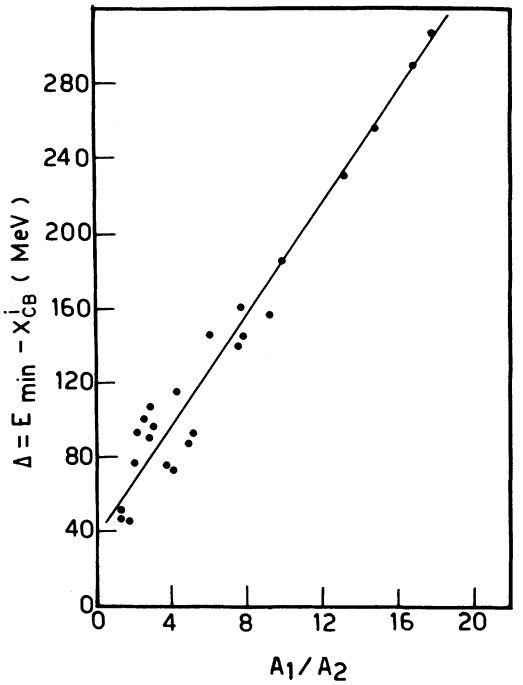

FIG. 8. The relation between $E_{min}-X^i_{CB}$ of A_1/A_2 for all reactions in Table I of Ref. 10. E_{min} is determined by using Eq. (18). This relation could be approximated to the straight line shown in the figure.

Ref. 10—where $E > E_{min}$ and to study the variation of γ_{up}—corresponding to the upper critical angular momentum—we consider the reactions where the incident energy is larger than E_{min}. For each reaction the empirical value of γ_{low} is determined using Eqs. (28)–(30) and the lower critical angular momentum is calculated. The value of γ_{up} is obtained by the fitting process in which γ_{up} is varied in steps of 0.01 until the critical angular momentum agrees with the experimental value. The calculated values of the critical angular momentum are plotted versus the experimental values and the results are represented by the hollow circles in Fig. 5. More experimental data are necessary to obtain a relation for γ_{up} similar to the empirical relation obtained for γ_{low}.

In the case of Kr induced reactions, the values of the incident energies for the reactions in Ref. 10 are smaller than the corresponding E_{min}. The values of η and γ_{low} which are used to obtain agreement between the experimental and calculated values of the critical angular momentum for different reactions are given in Table I.

From this table it is clear that the outgoing drops are nearly undeformed and the energy dissipated during collision is small. This means that the strong Coulomb repulsion causes separation to occur in the early stages after the formation of the composite system. The energy loss during the reaction is given by the difference in the rotational energies at collision and separation.

In the above consideration the effect of the nuclear shell on the deformation of the nuclei is neglected.

From the results some remarks may be made:

(1) The deformation energy plays an important role in the energy dissipation during collision. For example, in the reaction Ar + Ho at $E = 241$ MeV it was found if η in Eq. (13) equals 0.5, 0.6, or 0.7, no fitting is obtained between the experimental and calculated value of the critical angular momentum. When $\eta = 0.8$, the deformation energy was found to be equal to 23 MeV, while the energy dissipated due to friction and viscosity—i.e., $(1 - \eta)E$—is 48.2 MeV. When $\eta = 0.9$, the deformation energy—at the same incident energy—is 47.1593 MeV, while the energy dissipated during collision is 24.1 MeV. The importance of deformation energy was clarified in Ref. 10.

(2) Separation due to vibration is more important for collision with small energies, while separation due to rotation is more important for incident energies well above the Coulomb barrier; e.g., for $^{20}Ne + ^{27}Al$, if the cross sections for events where separation occurs due to rotation only and due to vibration only are given by

$$\sigma_1 = \pi\lambda^2 (l_{gr}^2 - (l_{crit}^{up})^2, \tag{31}$$

$$\sigma_2 = \pi\lambda^2 (l_{crit}^{up})^2, \tag{32}$$

respectively.

TABLE I. Values of the parameters η and γ_{low} which give agreement between the experimental and calculated values of the critical angular momentum for krypton induced nuclear reactions.

Reaction	E (c.m.) (MeV)	γ_{low}	η	$l_{exp,crit}$ ($\hbar$)	$l_{th,crit}$ ($\hbar$)
$^{84}Kr + ^{165}Ho$		1	0.96		82.73
	326	1.006 6	0.97	80	80
		1.015 24	0.98		80
		1.023 6	0.99		80
$^{84}Kr + ^{209}Bi$	358	1	0.99	36	45.44
$^{84}Kr + ^{238}U$	371	1	0.99	20	48.752

Calculating l_{crit}^{up} and l_{crit}^{low} as stated before, it was found that at 79 MeV σ_1/σ_2 equals 0.011 966 and at 120 MeV σ_1/σ_2 equals 0.4858. This implies that separation due to vibration is equivalent to quasifission which occurs for small partial waves[11] and separation due to rotation is equivalent to the deep inelastic collisions which occur at higher energies than quasifission.[32] The minimum energy necessary to produce separation due to rotation, E_{min}, may be taken as the limiting bombarding energy below which deep inelastic collisions do not occur.

(3) The deformation corresponding to separation due to vibration is always found to be larger than that when separation is due to rotation. The energy loss is larger in the former case.

(4) This model may provide an explanation for the presence of negative scattering angles in heavy ion induced reactions.[33,34] For incident energies near the Coulomb barrier, separation occurs due to vibration (quasifission); hence the angular momentum of the unstable composite system is small and hence the outgoing particle is scattered in the backward direction.

V. CONCLUSION

A simple model is proposed to explain deep inelastic and quasifission reactions. According to this model a formula for the critical angular momentum for complete fusion between target and projectile is obtained, which gives acceptable results compared to the experimental data. This model gives an idea about the deformation that occurs in the interacting nuclei especially when separation occurs due to vibration. The minimum bombarding energy below which separation due to rotation does not occur is also calculated.

[1]M. Lefort, G. Ngo, J. Peter, and B. Tamain, Nucl. Phys. A216, 166 (1973).
[2]F. Hanappe *et al.*, Phys. Rev. Lett. 32, 738 (1974).
[3]A. G. Artukh *et al.*, Nucl. Phys. A215, 91 (1973).
[4]B. Gatty *et al.*, Z. Phys. A 273, 65 (1975); Nucl. Phys. A253, 511 (1975).
[5]R. Babinet *et al.*, Nucl. Phys. A296, 160 (1978).
[6]F. Plasil *et al.*, Phys. Rev. Lett. 40, 1164 (1978).
[7]R. Vandenbosch *et al.*, Phys. Rev. C 17, 1672 (1978).
[8]J. R. Huizenga *et al.*, Phys. Rev. Lett. 37, 885 (1976).
[9]C. Volant *et al.*, Nucl. Phys. A238, 120 (1975).
[10]K. Siwek-Wilczynska and J. Wilczynski, Nucl. Phys. A264, 115 (1976).
[11]M. Lefort, Phys. Rev. C 12, 685 (1975).
[12]J. Wilczynski, Nucl. Phys. A216, 386 (1973); Phys. Lett. 47B, 484 (1973).
[13]R. Bass, Phys. Lett. 47B, 139 (1973).
[14]J. Galin *et al.*, Phys. Rev. C 9, 126 (1974).
[15]D. Horn, A. J. Ferguson, and O. Häusser, Nucl. Phys. A311, 238 (1978).
[16]J. P. Bondorf, M. I. Sobel, and D. Sperber, Phys. Rep. 15C, 84 (1974).
[17]D. Gross and H. Kalinowski, Phys. Lett. 48B, 302 (1974).
[18]J. Blocki, J. Randrup, W. J. Swiatecki, and C. F. Tsang, Ann. Phys. (N.Y.) 105, 427 (1977) and references therein; J. Randrup and J. S. Vaagen, Phys. Lett. 77B, 170 (1978).
[19]E. Seglie, D. Sperber, and A. Sherman, Phys. Rev. C 11, 1227 (1975).
[20]R. Bass, Phys. Rev. Lett. 39, 265 (1977).
[21]J. R. Birkelund and J. R. Huizenga, Phys. Rev. C 17, 126 (1978).
[22]J. R. Birkelund, J. R. Huizenga, J. N. De, and D. Sperber, Phys. Rev. Lett. 40, 1123 (1978).
[23]J. P. Bondorf, J. R. Huizenga, M. I. Sobel, and D. Sperber, Phys. Rev. C 11, 1265 (1975).
[24]C. Y. Wang, Phys. Lett. 61B, 321 (1976).
[25]J. Randrup, Ann. Phys. (N.Y.) 112, 356 (1978).
[26]G. Wolschin, Nucl. Phys. A316, 146 (1979).
[27]J. S. Sventek and L. G. Moretto, Phys. Rev. Lett. 40, 697 (1978).
[28]S. Cohen, F. Plasil, and W. J. Swiatecki, Ann. Phys. (N.Y.) 82, 557 (1974).
[29]P. R. Brazier-Smith, S. G. Jennings, and J. Latham, Proc. R. Soc. London A326, 393 (1971).
[30]S. G. Bradley and C. D. Stow, Philos. Trans. R. Soc. London, Ser. A 287, 635 (1978).
[31]J. R. Adam, N. R. Lindblad, and C. D. Hendricks, J. Appl. Phys. 39, 5173 (1968).
[32]M. F. Rivet *et al.*, Nucl. Phys. A267, 157 (1977).
[33]L. G. Moretto, R. P. Babinet, J. Galin, and S. G. Thompson, Lawrence Berkeley Laboratory Report No. LBL-3444, 1974.
[34]W. Trautmann *et al.*, Phys. Rev. Lett. 39, 1062 (1977).